

Tomographic images of the Mediterranean basin obtained by spatial prediction (kriging)

José Badal[†], Javier Sabadell[†] and Francisco J. Serón[‡]

[†]Physics of the Earth, Ciencias-B, Universidad de Zaragoza, 50009 Zaragoza

[‡]Computation Sciences, CPS, Universidad de Zaragoza, 50015 Zaragoza

Abstract

The purpose of this work is to give briefly an overall view of the shear wave velocity structure of the lithosphere-asthenosphere system beneath the Mediterranean basin, providing new tomographic images obtained through a method of spatial prediction applied to a common database. The starting data are path-averaged Rayleigh-wave group velocities previously determined by standard digital filtering, and then inverted by a damped least-squares. We use an interpolation method as kriging, especially useful for analysing short-range variability between scattered points. The results are shown by means of characteristic seismic velocities belonging to a prefixed interval, and horizontal slices at increasing reference depths down to 200 km. The method has allowed us to constrain the sharply contrasting seismic velocity structure between neighbouring areas of the Mediterranean. The images reveal significant variations in velocity with depth, and lateral changes in the crust and uppermost mantle elastic structure emphasising the processes associated with the convergence of the Eurasian and African plates.

Key words: surface waves, kriging, tomography, Mediterranean basin

1. Database and data processing

On the basis of surface waves propagating at a regional scale, we considered a total of 42 regional earthquakes selected from the USGS catalogue with M_s values ≥ 4.5 and focal depths ≤ 40 km, that occurred during the period 1990-1993, which were recorded at seismic stations installed in the Mediterranean area. The data set for this study consists of almost 200 wave trains generated by regional events recorded at very broad-band stations (Figure 1, upper part) belonging to or cooperating with the MedNet project (Boschi et al., 1988; Giardini et al., 1992). Epicentral distances mainly range from 500 to 1,500 km

and the path coverage (Figure 1, lower part) is fairly good on account of the relevant seismicity of the area despite the irregular distribution of stations (Martínez et al., 1996).

Our work benefited from the constructive pre-processing of real data. The basic information consists of path-averaged group velocities of fundamental mode Rayleigh waves across the Mediterranean basin. Reliable source-receiver, group-velocity dispersion up to periods of 90 s was determined by moving-window analysis on the signal to obtain approximate group arrival times. Afterwards, a correction of the waveform using a time-variable filter was performed in order to measure with the least possible bias the dispersion of the wave train (Badal et al., 1990, 1992). In principle, the wavelengths used sample well depths down to 160 km or even more.

Starting from path integrals that are representative of group times, local group velocities for periods ranging between 10 and 90 s over the area covered by the seismic trajectories were mapped. This operation involving linear inversion of travel times, was made as a previous step to volumetric modelling, and performed by means of the method proposed by Ditmar and Yanovskaya (1987) and Yanovskaya and Ditmar (1990). More recent applications can be found in Lana et al. (1997, 1999) and Yanovskaya et al (1998, 2000). Figure 2 shows as an example the local group-velocity contour map for a reference period of 40 s. Most remarkable lateral changes in group velocity are found for short periods ≤ 40 s. Longer periods show smooth lateral changes. The velocity uncertainties do not exceed 0.09 km/s and mainly range from 0.04 to 0.07 km/s for all periods, even in those areas with the poorest path coverage, such as south of the central Mediterranean and easternmost part of the basin (Figure 1).

The local velocities were inverted to shear velocity-depth profiles at almost 450 grid points over the study region using damped least-squares. The compressional and shear velocities and densities given by the PREM model (Dziewonski and Anderson, 1981) were taken as initial model to carry out inversion for velocity structure. The stochastic inversion of all these local dispersion curves permits to obtain the respective 1-D velocity-depth models, and to regard this set as linear constraints on the averaged properties of the 3-D shear wave velocity distribution. The reliability of the inversion results was tested by comparing the observed dispersion with the theoretical dispersion obtained after solving the forward problem, and their resolution through the kernels of the resolution matrix (Badal et al., 1996). In our case both procedures illustrate the good quality of the solution down to 160 km and sometimes at greater depths.

2. Spatial prediction

Our working scheme involves inversion and then volumetric modelling. In this context volumetric modelling implies spatial prediction that we perform using an interpolation method as kriging. A brief description of the mathematical content of kriging is depicted in Serón et al. (2001), where exact-type methods and approximate methods to reconstruct 3-D Earth structures from irregularly sampled seismic data are briefly described and compared. From a theoretical viewpoint, kriging is based on the theory of regionalised variables (Davis, 1986). It is a distance weighting estimation method that takes advantage of the spatial characteristics of the local structure through the variogram function. When the variogram is well known and well behaved, the resulting estimate is stated to be the best, linear, unbiased estimate that can be calculated (Isaaks and Srivastava, 1989).

The weighted contribution of each scattered datum is controlled not only by its relative position respect to the estimation point, but also by the specific spatial properties of the data involved in the estimation (Krajewski and Gibbs, 1996). When applying this technique, a number of matrix calculations must be completed as follows. A set of simultaneous equations are set up, which calculate the mean square difference between all the possible pairs of data point values, giving a matrix that we refer as $[K]$. A second matrix $[M]$ is computed in order to calculate the mean square difference between each scattered point value and the point to be estimated. This calculation is carried out using values from the variogram. The imposition of normalised weights is performed by a Lagrangian coefficient. The equation

$$[K] = [M][\lambda]$$

is inverted to obtain the kriging weights λ_i for each scattered data point value. With these weights the velocity estimation can be performed through the equation

$$\tilde{\nu} = \sum_i \lambda_i \nu(x_i, y_i), \quad i = 1, \dots, n.$$

Kriging provides an estimate of the error and confidence interval for every one of the unknown points, an asset not provided by other interpolation procedures. This information reflects the density and distribution of control points, and the degree of spatial autocorrelation, and therefore is very useful to analyse the reliability of the process. The error map may also be used to determine where more information is needed, so that future sampling may be planned.

Among the positive aspects of this technique we can say the following advantages. Kriged weights result in mean square error that is equal to zero. Kriging can estimate beyond the minimum and maximum values of the scattered data. Kriging can model both regional trends and local anomalies. Kriging is a robust estimator. Despite the

model presented below is based on the same data as used by Martínez et al. (2000), these advantages make it in principle a better one than simply applying linear interpolation to space-distributed shear wave velocity. As for disadvantages, kriging is not easy to understand mathematically and needs experienced staff with geostatistical techniques.

Many types of kriging are available and are used in different situations. In this work we are chosen “ordinary kriging”. It is the most widely used type of kriging, and permits to estimate values when data point values vary or fluctuate around a constant mean value.

To substantiate the reliability of the results provided by the imaging technique that we use, to ensure that the method works well, we take into account two aspects related to our spatial interpolator: accuracy and computational efficiency. This task has extensively been developed by Serón et al. (2001). The accuracy and computational efficiency of the spatial interpolator used have numerically been tested by synthetic outputs from the reconstruction of specific volumes whose (geometrical and physical) characteristics are known. The outputs so obtained prove the reliability of the final solution. Relative errors due to the algorithm measured under the l1-norm, for all the numerical tests, are in all cases fewer than 2-3%. This is indeed important for interpretation, as even though the numerical error does not reflect the error due to scatter of real data, the structures given and interpreted below may be considered actually resolved.

3. Results and interpretation

We directly supply shear wave velocity values, instead of positive and negative velocity anomalies, in any case estimated with the help of an interpolator not used until now. The idea, according to our stated main objective, is to review the S-wave velocity patterns concerning the Mediterranean basin, to constraint the contrasting seismic velocity structure between neighbouring areas of the basin, and to enhance the most conspicuous structural features.

After computing a three-dimensional matrix of voxelized data and using a 3-D data visualisation system, we have got tomographic images regarding the S-wave velocity structure beneath the Mediterranean basin. The most outstanding results are shown in Figures 3 and 4. These views allow us to see inner structural details of the basin by means of characteristic seismic velocities belonging to a prefixed interval (Figure 3), and horizontal slices at gradually increasing depths down to 200 km (Figure 4).

Lower velocities than 3.9 km/s are found in the crust for approximate depths between 20 (western basin) and 35-45 km (eastern basin). The subcrustal structure shows velocities up to 4.7 km/s approximately and a complex geometry over the whole basin. Underlying the lithosphere, the low velocity channel of the asthenosphere shows velocities

between 4.1 and 4.4 km/s, and exhibits a complicated form on its upper part (Figure 3). All these constraints agree with velocity values given by Corchete et al. (1995) for the Iberian subcrustal lithosphere and asthenosphere, and by Martínez et al. (2000) for the Mediterranean.

All the horizontal depth sections reveal significant lateral changes in shear velocity, with smaller values for the eastern part and higher ones for the western part, the maximum differences (sometimes close to 1 km/s for instance at 25 km) corresponding to the eastern and western ends. This is a general pattern valid at least down to 65 km (Figure 4). For each reference depth, the highest velocities arise in the Balearic Sea extending to Sardinia, whereas the lowest velocities are detected in the Adriatic Sea and above all to east of Crete. As the depth increases, the lateral changes become smoother and relative high velocities appear near Sardinia and the Algerian coast (45 km). These features suggest a significant variation in the lithosphere structure -a thickening of the crust- going from the Iberian Peninsula, Corsica and Sardinia to the opposite end of the Mediterranean, to the Ionian Sea, Albania, Greece, Aegean Sea, Crete, south of Turkey and Cyprus. So, a thin crust (20 km) would characterise the Balearic Sea, the Ligurian-Provençal basin and the Tyrrhenian Sea, and a thicker crust (35 km) the rest of the Mediterranean basin more or less. A conspicuous feature defined by relative high velocities is observed in the Balearic area and particularly to south of the Balearic Sea (25 km). The contrast with the north Balearic Sea is due to the thin continental crust underlying this zone opposite to the oceanic crust of the southern basin.

Since 65 km the velocity pattern changes notably. Areas of relative high velocity begin to appear in the central and eastern Mediterranean. Three specific high velocity areas are found in the Ionian Sea and south of the Adriatic Sea, between the Italian Peninsula and Greece, to south of the central basin, along the Algerian coast, and to west, near Corsica and Sardinia. Notable lateral changes in velocity arise at 95 km with a displacement of the highest velocities to east extending over the south Aegean, south Greece, Crete and reaching the Egyptian coast. These high velocities would be a consequence of the subduction of the eastern Mediterranean oceanic lithosphere dipping into the Hellenic Arc.

At greater depths of 130 and 160 km, the most evident variations in velocity take place in the western basin along a band from the Tunisian coast, through Sicily, to the Adriatic Sea, where we observe higher velocities in comparison with other neighbouring areas. Again, these high velocity values at deep levels would be a consequence of the collision processes associated with the convergence of the African and Eurasian plates and subduction under the Calabrian Arc. We observe again a conspicuous feature of the

north Balearic basin (95-130 km) consisting of the emergence of clearly high velocities. Now we are before the opposite case: low velocities in the south Balearic basin and high ones in the north basin. Despite this result can be explained by a deep beginning of the asthenosphere as one approaches the continental domain, since this small area is poorly covered by seismic paths, such a velocity contrast should be studied with special attention.

An interesting picture of the region as a whole in good agreement with tectonic regimes is as follows. On the basis of crustal velocities less than 3.9 km/s we can follow the changes in the location of the crust-mantle boundary and therefore the variable crustal thickness all over the Mediterranean region. We appreciate a 20 km thin crust in the western Balearic and Ligurian-Provençal basins and a gradually increasing thickness going to east, the crust reaching a maximum thickness of 45 km in the eastern Mediterranean, just between Crete and Cyprus (Figure 3). We observe likewise a crustal thickness of 35 km in the Ionian Sea, south Aegean Sea, and Peloponnisos, 30 km beneath the Greece Peninsula, and 30-35 km under the Italian Peninsula and Adriatic Sea. Assuming shear velocities between 4.1 and 4.4 km/s for the low velocity channel of the Mediterranean asthenosphere (Martínez et al., 2001), we can estimate that this gross layer extends beyond 200 km of depth varying its form and velocity structure from north to south and from west to east. The top of the asthenosphere is indeed irregular, albeit it is detected at an average depth of 75 km in the western basin (37°N-41°N). This depth becomes 150 km in the middle of the eastern basin (33°N-37°N). From south to north, the beginning of the asthenosphere varies from 150 to 90 km. Conspicuous features are the presence of materials characterised by relative high velocities at deep and variable levels affecting the lithosphere/asthenosphere transition in many places (Figure 3). We observe these materials down to 150 km in the middle of the eastern basin near the African coast (33-35°N), beneath Sicily (37°N), and to south and centre of the Italian Peninsula (39-41°N). The thicker lithosphere in these regions emphasises the processes associated with the convergence of the Eurasian and African plates: old subduction of the African lithosphere under Sicily, subduction of the Ionian lithosphere under the Calabrian Arc, and subduction of the eastern Mediterranean oceanic lithosphere dipping into the Hellenic Arc.

Acknowledgements

We acknowledge the Instituto Nazionale di Geofisica (Rome, Italy) for the facilities given for obtaining seismic records from MedNet broad-band stations. We are also grateful to M.D. Martínez and X. Lana of the Universidad Politécnic de Cataluña for the pre-processing of real data. Helpful comments from anonymous reviewers are gratefully acknowledged. The Dirección General de Investigación of the Ministerio de Ciencia y Tecnología, Spain, Project REN2000-1740-C05-04, supported this research.

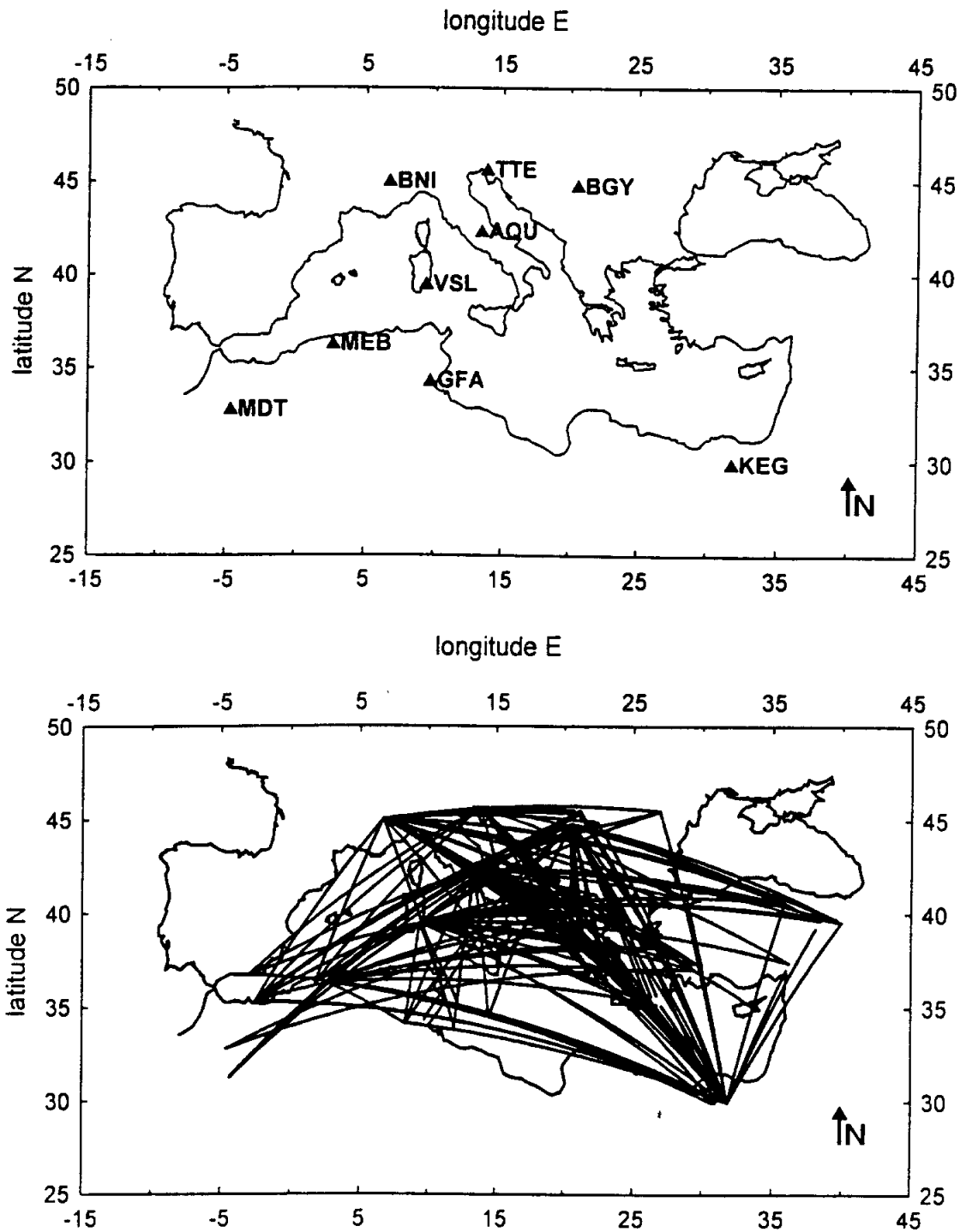


Figure 1.—Geographical location of the MedNet broad-band stations (small triangles) around the study region: the Mediterranean basin (upper part). Path coverage of the area for Rayleigh wave group velocity measurements depicted by great circles connecting epicentres to broadband stations (lower part).

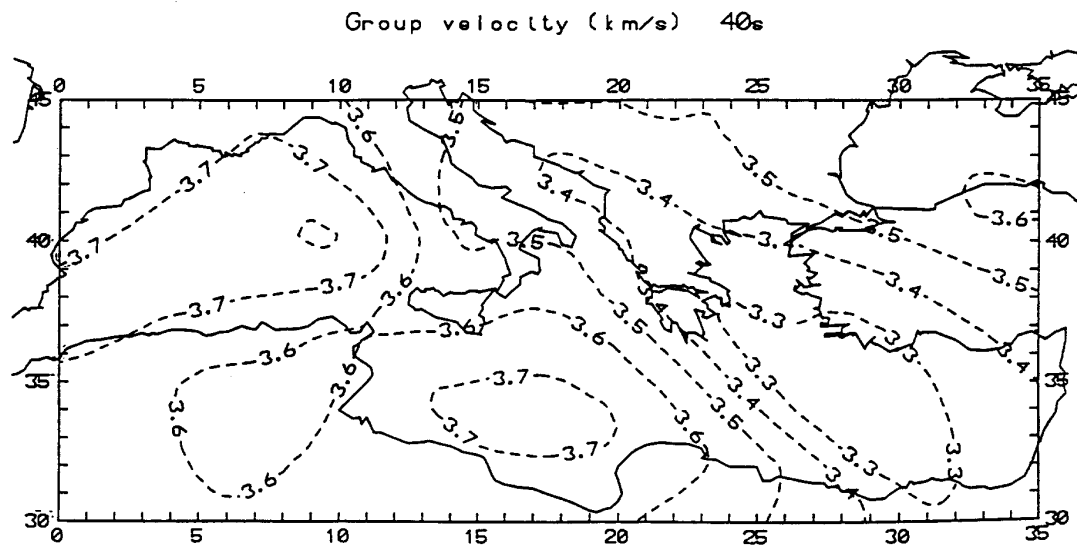


Figure 2.—Contoured local group-velocity pattern for the Rayleigh fundamental mode of 40 s propagating across the Mediterranean basin. Velocities in km/s. Isolines have been drawn in order to ensure clarity.

References

- [1] BADAL, J., V. CORCHETE, G. PAYO, J. A. CANAS, L. PUJADES and F. J. SERÓN (1990): Processing and inversion of long-period surface-wave data collected in the Iberian Peninsula, *Geophys. J. Int.*, **100**, 193-202.
- [2] BADAL, J., V. CORCHETE, G. PAYO, F. J. SERÓN, J. A. CANAS, and L. PUJADES (1992): Deep structure of the Iberian Peninsula determined by Rayleigh wave velocity inversion, *Geophys. J. Int.*, **108**, 71-88.
- [3] BADAL, J., V. CORCHETE, G. PAYO, L. PUJADES and J. A. CANAS (1996): Imaging of shear-wave velocity structure beneath Iberia, *Geophys. J. Int.*, **124**, 591-611.
- [4] BOSCHI, E., D. GIARDINI, A. MORELLI, G. ROMEO and Q. TACCETTI (1988): MedNet, The Italian broad-band seismic network for the Mediterranean, in *Workshop on Broad-Band Downhole Seismometers in the Deep Ocean*, edited by G. M. PURDY and A. M. ZIEWONSKI, Woods Hole Oceanographic Institute, MA, pp.116-124.
- [5] CORCHETE, V., J. BADAL, F. J. SERÓN and A. SORIA (1995): Tomographic images of the Iberian subcrustal lithosphere and asthenosphere, *J. Geophys. Res.*, **100**, 24133-24146.
- [6] DAVIS, J. C. (1986): *Statistics and Data Analysis in Geology*, Wiley, New York.
- [7] DITMAR, P. G. and T. B. YANOVSKAYA (1987): Generalization of the Backus-Gilbert method for estimation of lateral variations of surface wave velocities, *Physics of the Solid*

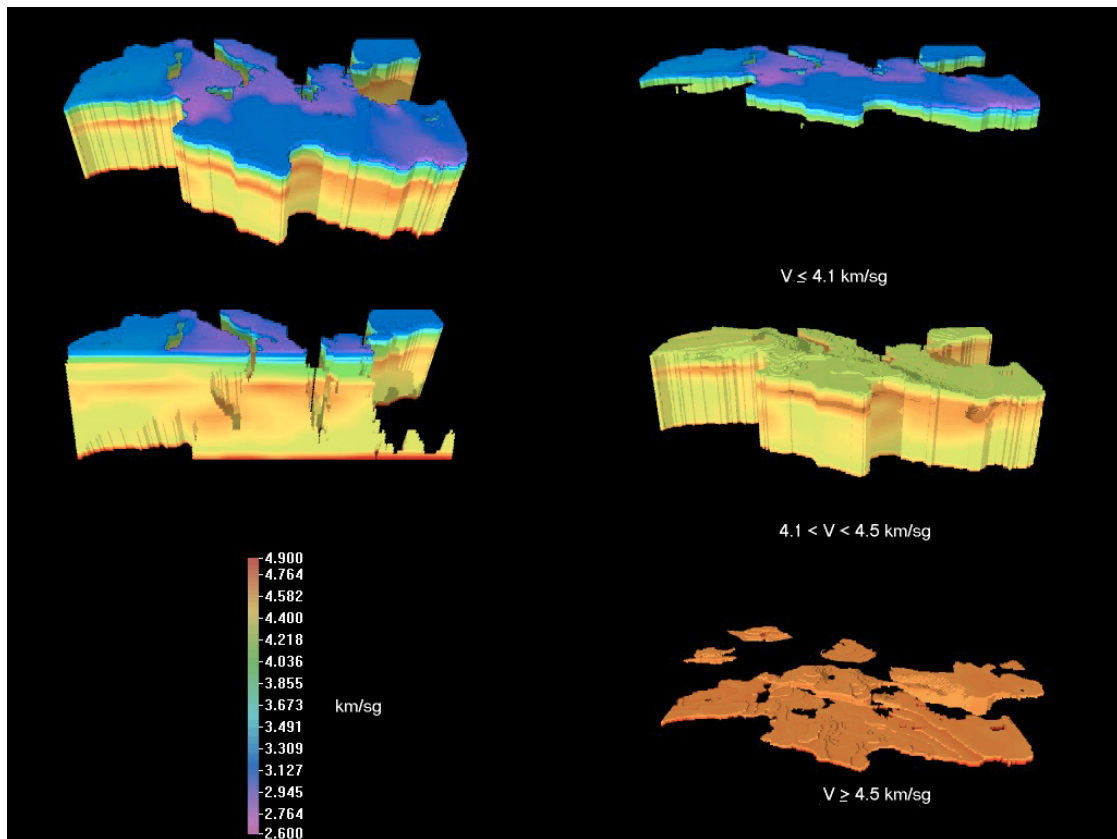


Figure 3.—Three-dimensional tomographic images of the Mediterranean basin as defined by characteristic shear velocity ranges. From top to bottom: ≤ 4.1 km/s, 4.1-4.5 km/s, ≥ 4.5 km/s. Materials connected with a specific velocity interval are thereafter displayed within a transparent volume representing the probed domain. An overall view together with an east-west vertical cross section of the basin (left side) images the shear-wave velocity structure of the lithosphere-asthenosphere system.

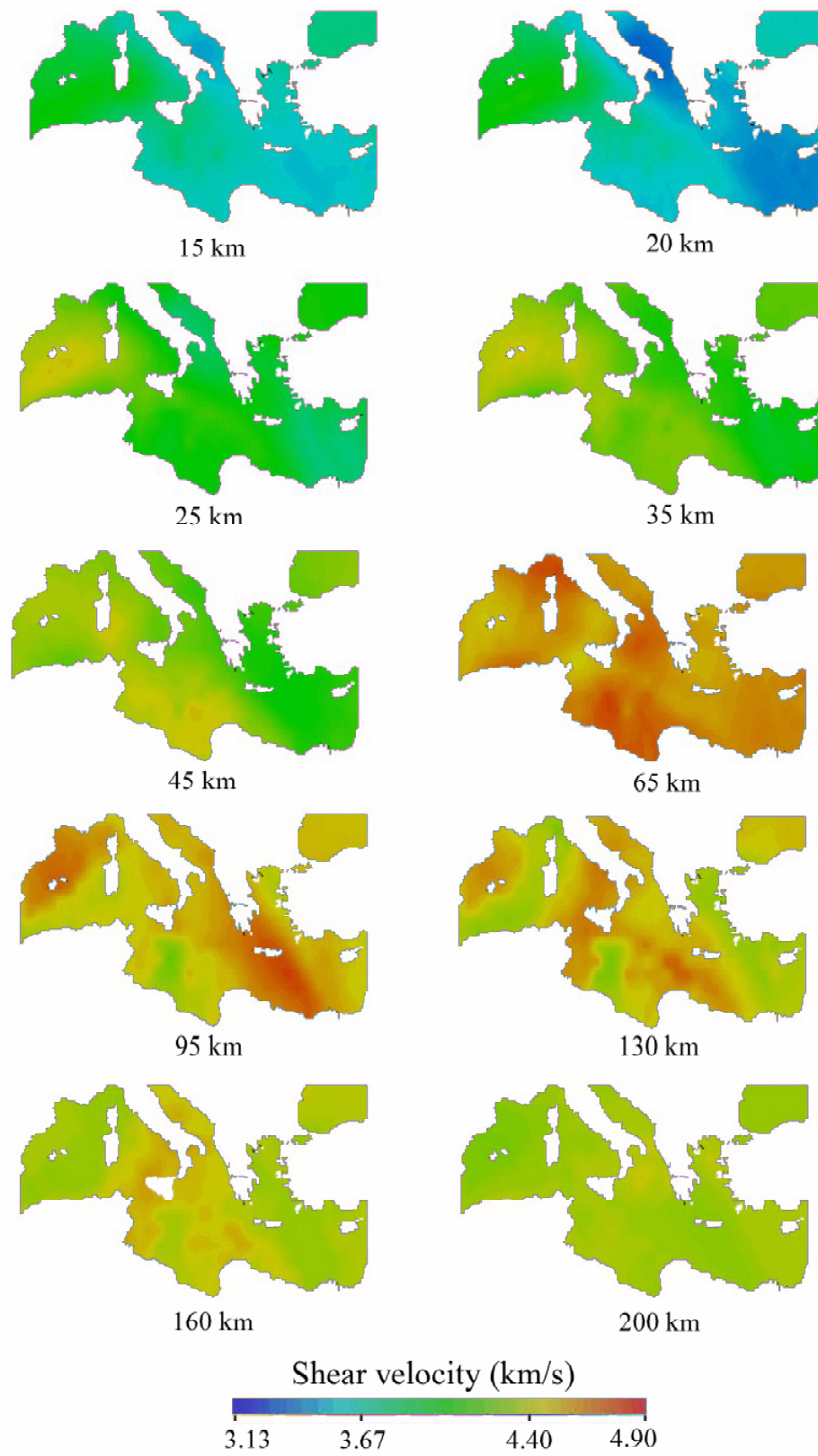


Figure 4.—Horizontal depth sections showing S-wave velocity panoramas for the structure under the Mediterranean Sea at different reference depths (from 15 to 200 km). Each coloured image represents the sea area outlined around by the European (north) and African (south) coasts. These pictures were obtained through spatial prediction by kriging, and obviously permit to appreciate the variations in velocity both laterally and with depth.

Earth, Izvestia Acad. Sci. USSR, **23** (6), 470-477.

- [8] DZIEWONSKI, A. M. and D. L. ANDERSON (1981): Preliminary Reference Earth model, *Phys. Earth Planet. Inter.*, **60**, 297-356.
- [9] GIARDINI, D., E. BOSCHI, S. MAZZA, A. MORELLI, D. BEN SARI, D. NAJID, H. BENHALLOU, M. BEZZEGHOUD, H. TRABELSI, M. HFAIDH, R. M. KEBEASY and E. M. IBRAHIM (1992): Very-broad-band seismology in Northern Africa under the MedNet project, *Tectonophysics*, **209**, 17-30.
- [10] ISSAKS, E. H. and R. M. SRIVASTAVA (1989): *An Introduction to Applied Geostatistics*, Oxford University Press, New York.
- [11] KRAJEWSKI, S. A. and B. L. GIBBS (1996): *Understanding Contourin*, Industrial Ergonomics, Inc., Colorado.
- [12] LANA, X., G. FERNÁNDEZ MILLS, J. BADAL and J. A. CANAS (1997): Objective regionalization of Rayleigh wave dispersion data by clustering algorithms, *Geophys. J. Int.*, **129**, 421-438.
- [13] LANA, X., O. CASELLES, J. A. CANAS, J. BADAL, L. PUJADES and M. D. MARTÍNEZ (1999): Anelastic structure of the Iberian Peninsula obtained from an automatic regionalization algorithm and stochastic inversion, *Tectonophysics*, **304**, 219-239.
- [14] MARTÍNEZ, M. D., X. LANA, J. BADAL and J. A. CANAS (1996): Improvements on the MedNet broadband network from the viewpoint of tomographic studies, *Geophys. Res. Lett.*, **23**, 2041-2044.
- [15] MARTÍNEZ, M. D., X. LANA, J. A. CANAS, J. BADAL and L. PUJADES (2000): Shear-wave velocity tomography of the lithosphere-asthenosphere system beneath the Mediterranean area, *Phys. Earth Planet. Inter.*, **122**, 33-54.
- [16] MARTÍNEZ, M. D., X. LANA, J. A. CANAS and J. BADAL (2001): Objective regionalization of Rayleigh wave dispersion data by clustering algorithms, *Tectonophysics*, **330**, 245-266.
- [17] SERÓN, F. J., J. I. BADAL and F. J. SABADELL (2001): Spatial prediction procedures for regionalization and 3-D imaging of Earth structures, *Phys. Earth Planet. Inter.*, **123**, 149-168.
- [18] YANOVSKAYA, T. B. and P. G. DITMAR (1990): Smoothness criteria in surface wave tomography, *Geophys. J. Int.*, **102**, 63-72.
- [19] YANOVSKAYA, T. B., E. S. KIZIMA and L. M. ANTONOVA (1998): Structure of the crust in the Black Sea and adjoining regions from surface wave data, *J. Seismol.*, **2**, 303-316.

- [20] YANOVSKAYA, T. B., L. M. ANTONOVA and V. M. KOZHEVNIKOV (2000): Lateral variations of the upper mantle structure in Eurasia from group velocities of surface waves, *Phys. Earth Planet. Inter.*, **122**, 19-32.